phys. stat. sol. (a) 48, 313 (1978)

Subject classification: 1.5 and 3; 2; 22.1.2

IBM Thomas J. Watson Research Center, Yorktown Heights[1])

Crystallization of Amorphous Silicon Films

By

U. KÖSTER[2])

Kinetics and morphology in crystallization of unsupported amorphous silicon films are investigated by hot stage transmission electron microscopy. Crystallization occurs by thermally activated nucleation and growth processes; activation energies of 470 kJ/mol for nucleation and 280 kJ/mol for growth are obtained. Nucleation rates are observed to increase with annealing time, whereas the growth rate depends on the annealing temperature and the crystallographic growth direction.

Kinetik und Morphologie der Kristallisation amorpher Silizium-Schichten wird elektronenmikroskopisch untersucht. Die Kristallisation erfolgt über thermisch aktivierte Keimbildung und Wachstum, wobei die Aktivierungsenergie mit 470 kJ/Mol für die Keimbildung und 280 kJ/Mol für das Wachstum bestimmt werden. Die Keimbildungsrate nimmt während isothermer Temperung zu; die Wachstumsgeschwindigkeit hängt dagegen nur von der Temperungstemperatur und der kristallographischen Wachstumsrichtung ab.

1. Introduction

The current interest in low-cost silicon solar cells has stimulated considerable research on polycrystalline silicon layers. Growing large silicon grains from amorphous silicon films is considered as a promising approach for the fabrication of such low-cost solar cells [1, 2]. Very little, however, is known so far on the crystallization behaviour of amorphous silicon films.

Crystallization of amorphous silicon films has been reported to occur in the 450 to 700 °C temperature range [3 to 6]. According to Blum and Feldmann [4, 5], the time for half the volume of the sample to become crystallized in the 550 to 700 °C temperature range, was found to follow the equation

$$t = t_0 \exp \frac{Q_0}{RT}$$

with $t_0 = 6 \times 10^{-15}$ s and $Q_0 = 320$ kJ/mol. For this investigation the crystallization process has been followed by observing optical transmission changes in the amorphous films as they were heated at various temperatures. The activation energy, therefore, reflects a certain combination of the nucleation and the growth activation energies and was found to be less than the activation energy for self-diffusion in silicon (380 kJ/mol). Hot-stage electron microscopy by Köster and Weiß [6] showed that crystallization occurs by nucleation and growth processes.

The purpose of this paper is to carry out a systematic study on nucleation and growth during crystallization of unsupported amorphous silicon films using hot-stage transmission electron microscopy. The information should be useful for growing large silicon grains by the crystallization of amorphous films.

[1]) Yorktown Heights, New York 10598, USA.

[2]) Present and permanent address: Institut für Werkstoffe, Ruhr-Universität Bochum, D-4630 Bochum 1, BRD.

2. Experimental Procedure

Thin amorphous silicon films were prepared by electron beam evaporation. The pressure during the deposition with a rate of about 0.4 nm/s was less than 4×10^{-4} Pa. The films deposited onto freshly cleaved NaCl crystals which were kept at room temperature throughout the evaporation had thicknesses in the range from 0.1 to 0.5 μm.

After evaporation the silicon films were removed from the substrate by dissolving the salt and floated onto molybdenum or tungsten electron microscope grids. The structure and annealing behaviour were investigated by hot-stage transmission electron microscopy in a Philips EM 301 electron microscope operated at 100 kV. For longer annealing times the samples used for TEM observations were annealed in a tube furnace flowing with dry helium.

3. Experimental Results

In the temperature range from 550 to 750 °C crystallization has been observed to occur by nucleation and growth processes. Fig. 1 shows a typical micrograph of this crystallization process. Crystallites are usually lens-shaped and contain a very high density of dislocations, twins, and stacking faults. Streaks and additional spots in the diffraction pattern are due to these lattice defects. The typical structure can be thought to be a lens-shaped crystal with a (011) plane parallel to the film surface with the [21$\bar{1}$] as the fastest growing direction. A remarkable feature of these crystals is the presence of stacking fault bundles and/or twins parallel to the fastest growing direction. A strong tendency for branching in other coplanar ⟨211⟩ directions has also been observed.

The growth rate (Fig. 2) in ⟨211⟩ directions has been found to be temperature dependent, but it is constant during isothermal annealing and is independent on film thickness. All these results were observed at least in the thickness range from 150 to 350 nm. The growth rate increases from about 8×10^{-10} cm/s at 550 °C to about 4×10^{-7} cm/s at 700 °C.

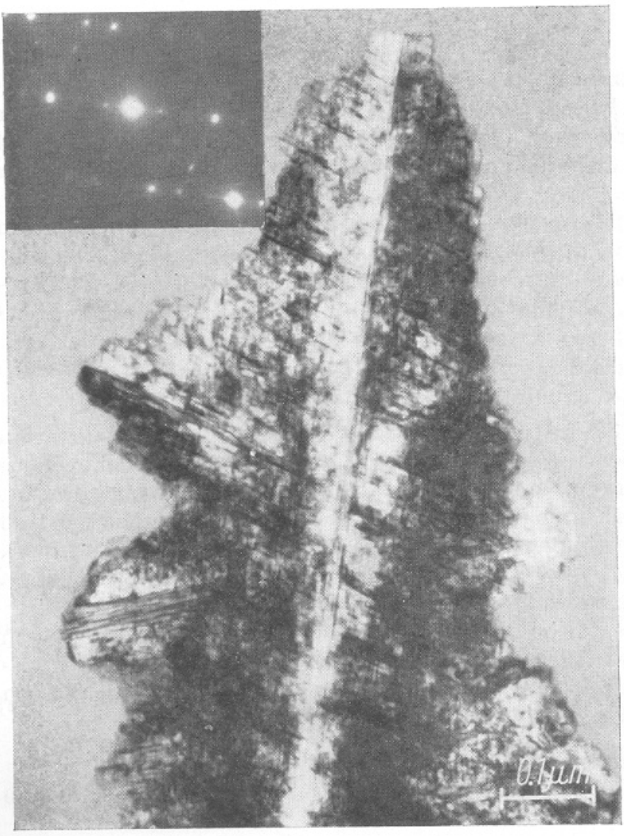

Fig. 1. Crystallization of amorphous silicon at 700 °C

Fig. 2. Temperature dependence of the growth rates during crystallization of amorphous silicon; thickness 0.15 to 0.35 μm ($u \sim \exp(-Q/RT)$, $Q \approx 280$ kJ/mol)

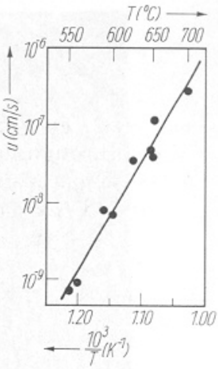

Nucleation rates have been observed to be time dependent (Fig. 3); they increase with annealing time. The rates calculated from the size of crystals assuming constant growth rates are in relatively good agreement with those measured by counting the number of crystals after different annealing periods. A step-wise annealing treatment of the same specimen, however, produces different results.

The very high heating rates that are required to achieve a total crystallization at higher temperatures and to avoid any crystallization during the temperature rise, can be produced by electron beam heating. The typical structure found after such heating (Fig. 4) consists of a fine-grained central area surrounded by large crystals formed in radial directions and a number of concentric crystalline shells. The length of the radial crystals and the number of the concentric shells increase with electron beam intensity and film thickness. The electron beam diameter has the size about the central fine-grained area. The radial crystals (Fig. 5a) grow usually into ⟨200⟩ directions containing a relatively low density of defects. Some crystals have been found with an extremely high density of stacking faults growing into ⟨211⟩ directions (Fig. 5b). The orientation of the crystalline shells of about 0.5 to 2 μm in width (Fig. 6) is given by the (110) plane parallel to the film surface and the [002] direction tangential to the rim. The dislocation density increases in each shell from the inner to the outer rim. As shown in Fig. 6b crystallization of a new shell starts near the point where the old one has grown together. Near the interface between the concentric shells and the amorphous matrix (Fig. 6c) crystallization morphology changes to that known from hot-stage electron microscopy at lower temperatures (see Fig. 1).

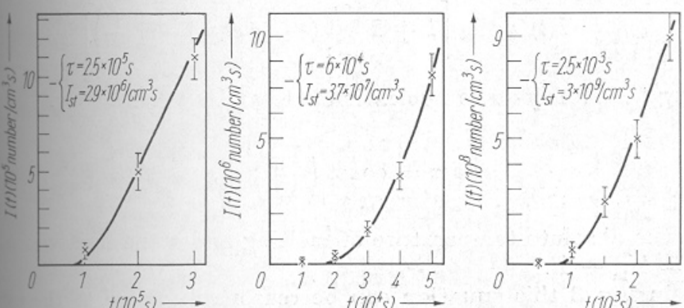

a b c

Fig. 3. Nucleation rates during crystallization of amorphous silicon at various temperatures a) $T = 551$, b) 588, c) 647 °C

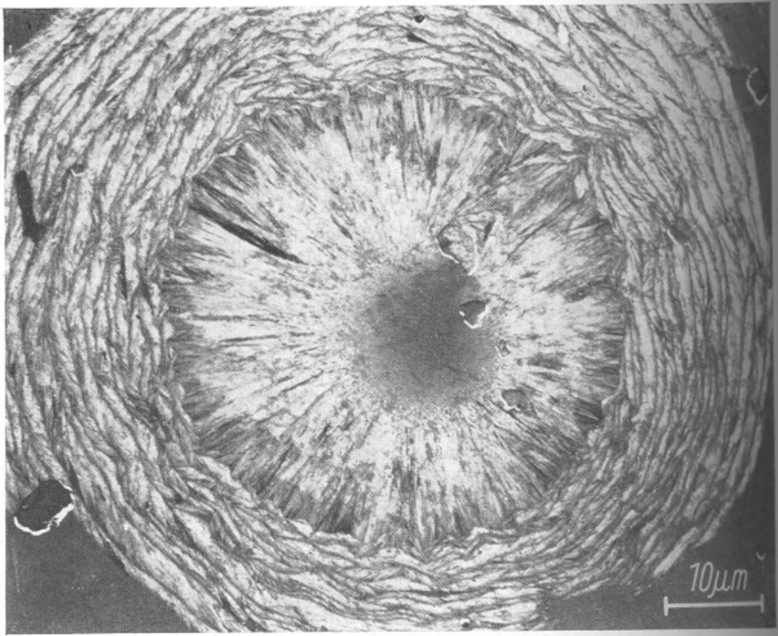

Fig. 4. Crystallization of amorphous silicon produced by electron beam pulse heating

4. Discussion

In nucleation theory, usually, it is assumed that a steady-state concentration clusters exists at all the times. However, at the very beginning of crystalliza there must be a finite period during which this steady-state concentration is be established. Such transient or time-dependent nucleation has been predicted crystallization of amorphous materials with high viscosity and has been reported some oxide glasses [7]. An approximate expression for the transient nucleation $I(t)$ derived by Kashchiev [8] is given by the following equation:

$$I(t) = I_{st} \left[1 + 2 \sum_{n=1}^{\infty} (-1)^n \exp \left(-n^2 \frac{t}{\tau} \right) \right]$$

with I_{st} being the steady-state nucleation rate and τ the time lag. The time lag given by

$$\tau = \text{const} \left(\frac{T_m}{\Delta T} \right)^2 \eta ,$$

where T_m is the absolute temperature of melting and η the melt viscosity at cooling $\Delta T = T_m - T$.

As shown in Fig. 3 this equation can be reasonably fitted to the experiment observed nucleation rates. By such fitting one obtains values for the time lag the steady-state nucleation rate I_{st}. The time lag τ was found to decrease with creasing temperature significantly from 2.5×10^5 s at about 550 °C to 2.5 × at about 650 °C. The temperature dependences of the steady-state nucleation I_{st} and the crystal growth rate u can be described by Arrhenius-type equations activation energies of 470 kJ/mol for nucleation and 280 kJ/mol for growth. Using

Fig. 5. Structure of silicon crystals in the radial grain area (the arrows indicate the growth directions). a) ⟨200⟩ growth direction, b) ⟨211⟩ growth direction

these data on nucleation and growth the time for half the volume of a film to be crystallized can be estimated. Calculated periods of 140 h at 550 °C and 1 h at 6… are comparable to the values reported by Blum and Feldmann [4, 5] and give the same apparent activation energy of 320 kJ/mol which indeed reflects a combination of the activation energies for nucleation and for growth.

A very similar study on nucleation and growth rates but with amorphous germanium has been reported by Barna et al. [9]: These authors observed a very similar crystallization behaviour, except for the transient nucleation. As in silicon, both nucleation and crystal growth can be described by an equation of the Arrhenius type. Activation energies are much smaller with 250 kJ/mol for nucleation and 125 kJ/mol for growth. Nevertheless, actual nucleation and particularly growth rates are higher in silicon if one compares germanium to silicon, over temperature ranges scaled to their melting temperatures. This occurs as a result of a very high pre-exponential factor in the Arrhenius equation for growth of silicon crystals, indicating that the growth is probably the result of a coordinated jump of several atoms over the crystallization front.

So far we have no information on what nucleation sites are. Nucleation rates seem to be higher in thinner silicon films indicating some surface influence. These results, however, are not significant enough to draw any definite conclusion.

Silicon shows a much more pronounced crystallization morphology with growth in ⟨211⟩ directions than germanium [10]. This is probably due to the lower stacking fault energy of silicon, because for such fast propagation in ⟨211⟩ at least two twins parallel to this direction have been shown to be necessary [11]. The atomic plane of the surface of Si crystals has been found to be {110} planes. Comparing the surface energies of silicon [12], 1.23 J/m^2 for (111) planes with 1.51 J/m^2 for (110) planes, it is not possible to explain the observed preferential (110) orientation. Besides, such surface energies should be important only for nucleation at surfaces or for orientation selection during growth.

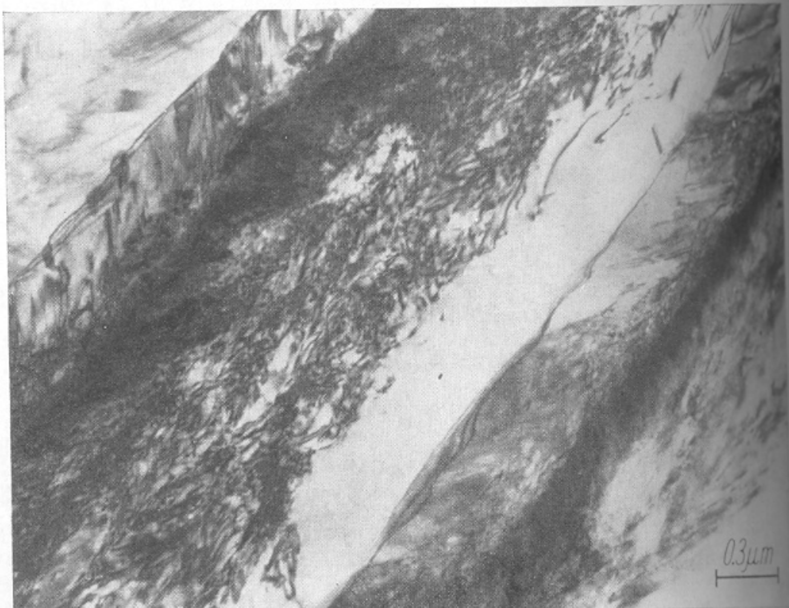

Fig. 6a

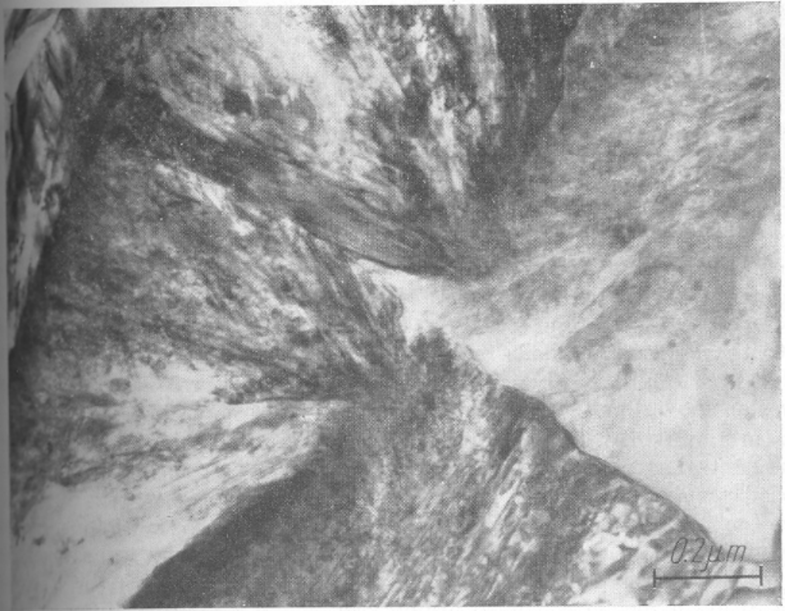

b

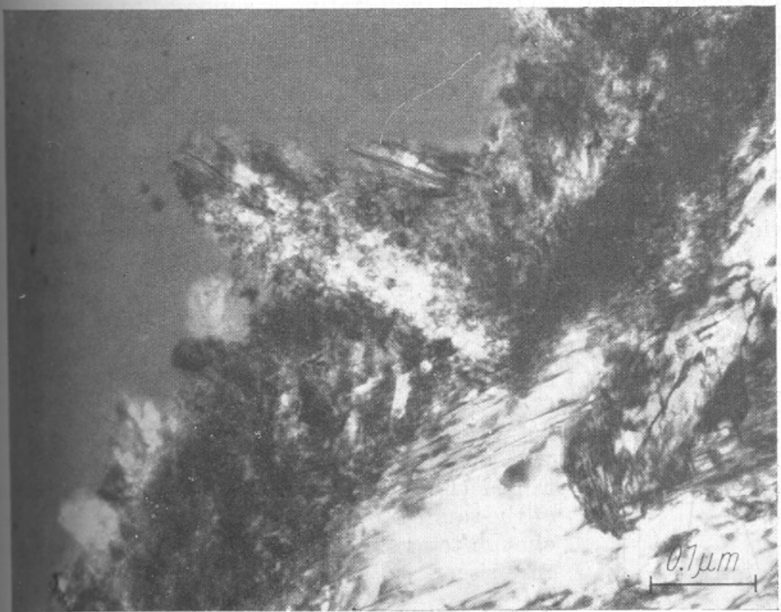

c

Fig. 4. Structure of silicon crystals in the crystalline shell area. a) Typical structure of a shell, b) nucleation of a new shell, c) transition from the shell area to the amorphous matrix

At higher temperatures or temperature gradients the fastest growth di… changes to ⟨200⟩ in both germanium [10] and silicon, giving rise to flat surfaces… grain boundaries perpendicular to the surface, which are approximately paral… the four {011} planes with parallel [200] growth axis. The reason for selecting… growth axis is not clear at the present time.

Such shell-like crystallization morphology[3]) as shown in Fig. 4 has been repo… earlier to occur during "explosive" or shock crystallization in thick amorph… antimony [13] and germanium films [14 to 16]. In those investigations the ex… rapid growth is explained by energy transfer of the heat of crystallization, how… the microstructure of the shells has not been analysed.

The concentric wavy marks observed by optical or scanning electron micro… were interpreted only as the result of the crumpling of the film by the stress… during the crystallization reaction. In our opinion the drastic change from the ra… grains to the crystalline shells in Fig. 4 and the formation of the shells can be… plained at least qualitatively using a schematical diagram of growth rates over… peratures as shown in Fig. 7: It is reasonable to assume that there is a strong… temperature gradient from the central area to the shell region produced by heat… from the central area heated by the electron pulse. The temperature distributi… be divided roughly into two regions: At temperatures higher than the critical… perature for maximum growth rate, growth will be accelerated into regions at l… temperatures giving rise to that fast radiate growth. At temperatures lower tha… critical value growth will be faster in areas with higher temperatures, i.e. near… rim of a Si grain just crystallized giving rise to the formation of the shell-like… phology.

During crystallization the critical temperature is supposed to appear in the tra… tion region between the radiate grains and the crystalline shells. Heat producti… to the latent heat of crystallization and heat loss by surface radiation will infl… the detailed temperature distribution [17]. For example, the relative heat los… to surface radiation will become smaller with increasing film thickness thus red… the temperature gradient. Therefore, in thicker silicon films radial crystals will… longer and the number of shells will increase.

With this knowledge on nucleation and growth rates one can discuss the possi… of growing large crystals from amorphous silicon films. For example, from Fi… the time for growing a crystal with about 1 μm length will be about 2.5 × 10… 700 °C. During this period, however, more than 10^{12} nuclei/cm^3 will have for… This implies that after a period for growing a crystal of only 1 μm length, every s… with about 1 μm diameter will contain at least one nucleus. Therefore, large s… grains grown by crystallization of amorphous silicon la… can be expected only by annealing at much higher te… peratures where the nucleation rate starts to decr… with temperature but a high growth rate can be m… tained (Fig. 7). Even under such conditions, the hea… of the sample to that temperature range has to occur… enough to avoid excessive nucleation during the temp… ture rise.

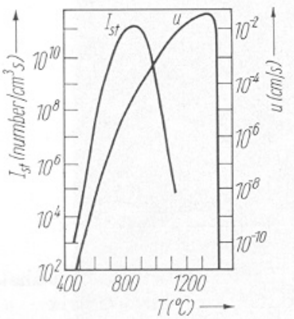

Fig. 7. Schematic diagram of nucleation and growth rates d… crystallization of amorphous silicon. The data from Fig. 2 and… extrapolated using classical nucleation and growth theori…

[3]) Very recently, the same crystallization morphology has been observed by Aleksandr… Edelman [18] after shock crystallization of SiO_2 and Si_3N_4.

Acknowledgements

author thanks D. Campbell for providing the Si films and is indebted to pbell, P. S. Ho, and K. N. Tu for helpful comments and discussions.

References

C. C. Fan and H. J. Zeiger, Appl. Phys. Letters **27**, 224 (1975).
L. Chu, H. C. Mollenkopf, and S. S. C. Chu, J. Electrochem. Soc. **123**, 106 (1976).
H. Brodsky, R. S. Title, K. Weiser, and G. D. Petit, Phys. Rev. B **1**, 2632 (1970).
A. Blum and C. Feldmann, J. non-crystall. Solids **11**, 242 (1972).
A. Blum and C. Feldmann, J. non-crystall. Solids **22**, 29 (1976).
Köster and P. Weiss, J. non-crystall. Solids **17**, 359 (1975).
Gutzow and S. Toschev, in: Adv. Nucleation Cryst. Glasses, Ed. L. L. Hench, Amer. Ceram. Soc., Columbus (Ohio) 1971 (p. 10).
Kashchiev, Surface Sci. **14**, 209 (1969).
Barna, P. B. Barna, and J. F. Pócza, J. non-crystall. Solids **8/10**, 36 (1972).
Köster, Acta metall. **20**, 1361 (1972).
R. Hamilton and R. G. Seidensticker, J. appl. Phys. **31**, 1165 (1960).
J. Jaccodine, J. Electrochem. Soc. **110**, 524 (1963).
Götzberger, Z. Phys. **142**, 182 (1955).
Takamori, R. Messier, and R. Roy, Appl. Phys. Letters **20**, 201 (1972).
Takamori, R. Messier, and R. Roy, J. Mater. Sci. **8**, 1809 (1973).
Mineo, A. Matsuda, T. Kurosu, and M. Kikuchi, Solid State Commun. **13**, 329, 1307 (1973).
Köster and P. Ho, unpublished results.
N. Aleksandrov and F. L. Edelman, Izv. Akad. Nauk. SSSR, Ser. fiz. **41**, 2310 (1977).

(Received May 5, 1978)